Journal of Inorganic Biochemistry 115 (2012) 138–147

Contents lists available at SciVerse ScienceDirect

Journal of Inorganic Biochemistry

journal homepage: www.elsevier.com/locate/jinorgbio

# Structural approaches to probing metal interaction with proteins

Lorien J. Parker [a,1,2], David B. Ascher [a,2], Chen Gao [a,2], Luke A. Miles [a,b,c,3], Hugh H. Harris [d,3], Michael W. Parker [a,c,*,3]

[a] Biota Structural Biology Laboratory, St. Vincent's Institute of Medical Research, 9 Princes Street, Fitzroy, Victoria 3065, Australia
[b] Department of Chemical and Biomolecular Engineering, The University of Melbourne, Victoria 3010, Australia
[c] Department of Biochemistry and Molecular Biology, Bio21 Molecular Science and Biotechnology Institute, The University of Melbourne, 30 Flemington Road, Parkville, Victoria 3010, Australia
[d] School of Chemistry and Physics, University of Adelaide, South Australia 5005, Australia

ARTICLE INFO

*Article history:*
Received 1 December 2011
Received in revised form 2 February 2012
Accepted 20 February 2012
Available online 3 March 2012

*Keywords:*
Amyloid precursor protein
Glutathione transferase
Insulin-regulated aminopeptidase
X-ray absorption spectroscopy
X-ray crystallography

ABSTRACT

In this mini-review we focus on metal interactions with proteins with a particular emphasis on the evident synergism between different biophysical approaches toward understanding metallobiology. We highlight three recent examples from our own laboratory. Firstly, we describe metallodrug interactions with glutathione S-transferases, an enzyme family known to attack commonly used anti-cancer drugs. We then describe a protein target for memory enhancing drugs called insulin-regulated aminopeptidase in which zinc plays a role in catalysis and regulation. Finally we describe our studies on a protein, amyloid precursor protein, that appears to play a central role in Alzheimer's disease. Copper ions have been implicated in playing both beneficial and detrimental roles in the disease by binding to different regions of this protein.

© 2012 Elsevier Inc. All rights reserved.

## 1. Introduction

Professor Hans Freeman AM FAA made a number of highly important contributions to bioinorganic chemistry, amongst which include setting up the first protein crystallography laboratory in Australia, being a strong advocate and supporter of synchrotron science and its applications in biology and using X-ray crystallography and other biophysical tools, such as X-ray absorption spectroscopy (XAS), to probe the function of blue copper proteins [1].

In this mini-review we highlight recent discoveries at St Vincent's Institute (Melbourne, Australia), one of the oldest protein crystallography centers in Australia [2], on metal interactions with proteins with a particular emphasis on the evident synergism between different biophysical approaches to understanding metallobiology. This review focuses on three biological systems: 1) glutathione S-transferases (GSTs) which normally function by recognizing foreign small molecule toxins in the body and causing them to be eliminated from the cell. Unfortunately, commonly used anti-cancer drugs such as cisplatin are also recognized as toxic and thus GSTs contribute to the resistance of such drugs; 2) insulin-regulated aminopeptidase (IRAP) which appears to be the target for small memory enhancing molecules. This aminopeptidase uses zinc for both catalysis and for regulating its activity; 3) amyloid precursor protein (APP) which appears to play a central role in Alzheimer's disease. Copper ions have been implicated in playing both beneficial and detrimental roles in the disease by binding to different regions of APP.

## 2. Glutathione S-transferase recognition of anti-cancer metallodrugs

### 2.1. Introduction

Glutathione S-transferases (GST) are a family of Phase II detoxification enzymes that function by catalyzing the conjugation reaction of glutathione (GSH) to small toxic molecules in the cell for subsequent removal [3–5]. The GST superfamily has been subdivided into at least twelve classes [6,7]. The first classes to be identified, and now the most studied, are the mammalian cytosolic classes termed pi, mu and alpha [8]. The prevalence of GSTs in disease states, together with evidence detailing their role in detoxification of cytotoxic compounds, has stimulated many investigations into the involvement of these enzymes in disease. GSTs have been implicated in the development of resistance by cells and organisms toward drugs, pesticides, insecticides, herbicides and antibiotics [9].

The human pi class GST (GSTP1-1) is often overexpressed in cancer tissues including those in the lung [10], colon [11,12], ovary [13],

* Corresponding author at: St. Vincent's Institute of Medical Research, 9 Princes Street, Fitzroy, Victoria 3065, Australia. Tel.: +61 3 9288 2480; fax: +61 3 9416 2676.
*E-mail address:* mparker@svi.edu.au (M.W. Parker).
[1] Present address: RIKEN Systems and Structural Biology Center (SSBC) 1-7-22, Suehiro-cho, Tsurumi-ku, Yokohama City, Kanagawa, 230-0045, Japan.
[2] These authors made equal contributions.
[3] Co-senior authors.

0162-0134/$ – see front matter © 2012 Elsevier Inc. All rights reserved.
doi:10.1016/j.jinorgbio.2012.02.015

testis [14], bladder [15], mouth [16] and kidney [17]. This overexpression has been associated with transformation to malignancy [11] and the adaptive resistance to anti-cancer drugs [18,19]. Inhibitors of GSTP1-1 have been used in clinical trials as adjuvants in cancer chemotherapy with limited success due to side-effects including toxicity. Ethacrynic acid (EA; Fig. 1A) has been identified as a potent inhibitor of GSTP1-1 and has been investigated as a potential therapeutic molecule [20,21]. Despite promising results the development of side-effects including dose limiting toxicities proved too severe to continue on with Phase II trials [22]. There is thus an urgent need for the design of new anti-cancer drugs that circumvent the development of GST-mediated resistance to treatment. Alternatively, GST inhibitor compounds that can be used as adjuvants in conjunction with current chemotherapy drugs represent another approach to evading or reducing the occurrence of GST-mediated resistance. We have used a combination of structural studies and biochemical approaches to investigate the

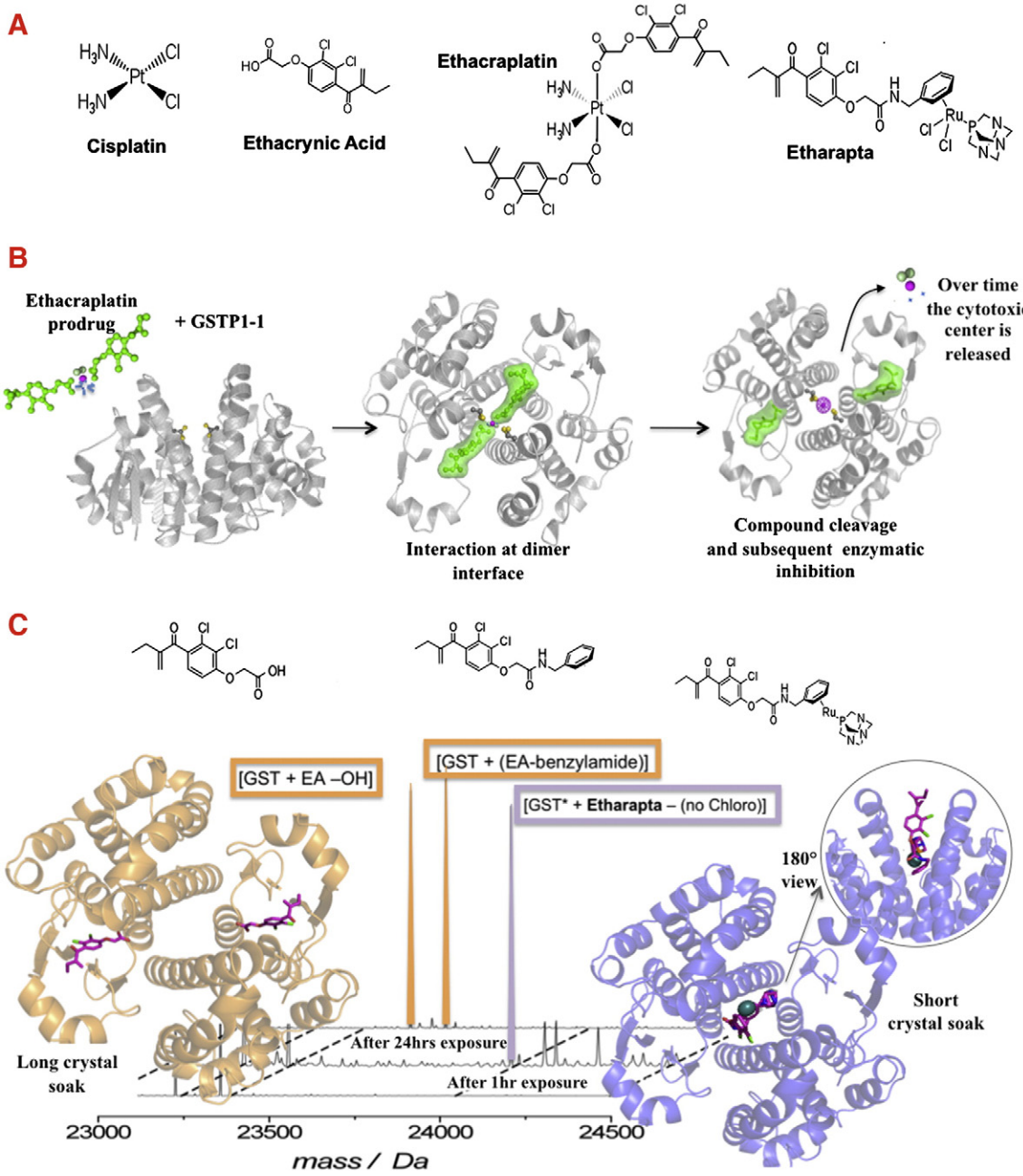


**Fig. 1.** Metal binding to GST. (A) Chemical structures of some metal-based drug and drug-like compounds that interact with GSTP1-1: cisplatin, ethacrynic acid, ethacraplatin and etharapta. (B) Overview of the proposed mechanism of GSTP1-1 interaction with ethacraplatin. EACPT is shown in ball-and-stick fashion with EA moieties represented by green sticks, the Pt center by a pink sphere and metal ligands by small spheres. GSTP1-1 is shown as gray ribbons. The intact compound is thought to bind at the dimer interface in a relatively symmetric manner. The compound is then cleaved and the EA moieties transverse to the substrate-binding site while the Pt center remains bound to the dimer interface via cysteine residues. At some point, the activated Pt(II) center is released. (C) Overview of the breakdown of etharapta over time as captured by X-ray crystallography and mass spectrometry. After 1 h exposure of GST to etharapta, an adduct corresponding to the GST–etharapta complex minus the chloro groups, is observed. This is represented on the right hand side of the figure by the purple peak in the spectra. The corresponding complex derived from the crystallographic data is shown as a purple ribbon structure. The etharapta molecule is colored as pink sticks with a green sphere representing the ruthenium center. Inside the circle is a close up view of crevice binding site at the dimer interface, rotated by 180°. On the left side of the figure, the adducts observed after longer exposure times are shown. The two orange peaks represent the complexes of GST plus the EA moiety (either as OH or benzylamide adducts), minus the Ru center and the PTA moiety. The corresponding crystallographic results are depicted by the orange ribbon structure showing the EA moieties (pink sticks) bound at the substrate binding sites. There is no longer anything bound at the dimer interface.

means by which GSTP1-1 is involved in resistance to metal-based chemotherapy treatment. This work is providing the basis for a structure-guided approach to developing new GST inhibitors that might overcome GST-mediated resistance.

### 2.2. Overcoming GST resistance — inhibition by the metallocomplex EACPT

Cisplatin (CPT; Fig. 1A), an FDA approved anti-cancer drug, is one of the most widely used cancer chemotherapeutic drugs used for the treatment of solid tumors [23–27]. The drug exerts it cytotoxicity through the formation of DNA inter- or intra-strand cross-links that affect both replication and transcription [28–30]. Unfortunately, recurrences of disease as well as resistance to treatment remain major limitations in cisplatin use [25].

GSTP1-1 has been shown to play a role in development of resistance to cisplatin treatment, which we have proposed is most likely through reduction of the amount of cisplatin that successfully reaches the nucleus. GSTP1-1's involvement in drug resistance has been supported through many observations that show that GST overexpression is associated with failure of therapy and poor patient survival in treatment of leukemias and solid tumors [31,32]. The enzyme is overexpressed in cisplatin-resistant cell lines [33,34] and inhibition of the enzyme has been shown to reverse resistance [35]. Furthermore, GSTP1-1 knockout mice are much more sensitive to the cytotoxic effects of cisplatin than their wild-type counterparts [36].

Strategies to overcome cisplatin drug resistance are urgently being sought. One such option is to design and build specific functionalities onto platinum compounds that either result in enhanced uptake via drug targeting (as seen for many platinum analogs) or that can inhibit the mechanisms by which resistance is occurring (*e.g.* by inhibiting enzymes such as GSTP1-1). Pt(II) complexes, such as cisplatin, are limited in their geometry and coordination number, and are thus severely restricted in their usefulness as leads to develop new, improved compounds. In addition, anti-cancer active Pt(II) complexes, especially cisplatin, are kinetically labile agents, which readily react with sulfur-containing biomolecules such as amino acids, GSH and proteins, including GSTs. This leads not only to the deactivation of the Pt(II) agent, but additionally to the production of side-effects caused by non-specific binding.

Recently, more chemically inert Pt(IV) complexes have been designed and are displaying encouraging results in the laboratory and in clinical trials as anti-cancer agents [37–41]. Pt(IV) complexes are generally octahedral in geometry and thus possess two extra ligand sites (compared to Pt(II) compounds) that can be selectively tailored to modify the pharmacokinetic properties of the compound (*e.g.* rate of reduction, lipophilicity, molecular targeting and microenvironment targeting) in order to reduce side-effects, increase activity and specifically target tumor sites. Additionally, the axial ligands themselves can be designed to confer additional cytotoxicity upon release [42].

Ethacraplatin (EACPT) is a Pt(IV) compound (Fig. 1A), designed by Dyson and co-workers, that was tailored to inhibit GST through its axial ligands while simultaneously releasing a cytotoxic platinum payload for DNA modification [42,43]. The compound has a Pt(IV) center with two ethacrynic acid (EA) ligands at the axial positions. They observed a 10-fold increase in GST inhibition compared to EA alone. Further, they found that EACPT was able to penetrate live mammalian cells and inhibit GST as well as inhibiting the cell viability of a panel of carcinoma cell lines. More recently, we reported the crystal structure of this compound bound to GSTP1-1 [44]. The Pt center was found bound to the thiols of the Cys101 residues at the dimer interface of the protein, rather than the expected substrate binding site (Fig. 1B). There was no extra electron density to suggest that the EA moiety was still attached to the Pt center at the dimer interface. However, density attributable to the two EA moieties was observed in the active site of each subunit. It appears that the EACPT molecule had been cleaved and bound to the enzyme as three separate moieties (Fig. 1B).

It was more difficult, however, to discern which ligands of the Pt(IV) center were displaced upon binding to the cysteine residues at the dimer interface. There was electron density for one small ligand, possibly a chloride or one of the amino groups. Molecular dynamics simulations suggested that the missing fourth ligand was most likely a hydroxyl, water or amine. EXAFS was then undertaken in a further attempt to resolve the identity of the third and fourth ligands. The extended X-ray absorption fine structure spectroscopy (EXAFS) experiments suggested that the platinum was bound to four sulfur or chlorine ligands. However, the interpretation was complicated due to the possibility of other sites of interaction for the Pt center (including an N-terminal methionine, an artifact of the recombinant expression, and another reactive cysteine residue, Cys47), and the inability of EXAFS analyses to distinguish sulfur from chlorine backscatterers so no concrete conclusions could be drawn. Our tentative reaction scheme for GSTP1-1 interaction with EACPT is shown in Scheme (1):

$$\mathrm{GST} + [\mathrm{Pt(IV)Cl_2(NH_3)_2EA_2}] \rightarrow \mathrm{GST}-[\mathrm{Pt(II)X_2}] + 2\mathrm{EA} \quad (1)$$
$$+2\mathrm{NH_3} \rightarrow \mathrm{GST}-[\mathrm{Pt(II)X_2}]-2\mathrm{EA}$$

where X represents ligands that are not definitely identified.

X-ray absorption near edge structure (XANES) analysis showed that the bound metal was clearly a Pt(II) species, whereas the parent EACPT had a Pt(IV) oxidation state. This showed that the Pt(IV) center was reduced to a Pt(II) in the presence of GSTP1-1.

The order of events leading to the breakdown of the EACPT complex is unclear although we speculate, based on extensive molecular modeling, that the intact molecule binds to the dimer interface and is subsequently cleaved by the protein, releasing the EA moieties that diffuse a few Å along a water-filled channel, toward the active site, where they bind to the enzyme in a manner that was observed previously in the crystal structure of the enzyme with ethacrynic acid (PDB ID: 2GSS; Fig. 1B; [45]). Mass spectrometry data also showed that the EACPT complex is stable for extended periods of time, suggesting that any cleavage of EACPT into its components is enzymatically driven [44]. The proposed cleavage mechanism and release of the ethacrynic acid moieties as determined through crystallographic, mass spectrometry, molecular modeling and XANES studies provide a molecular level explanation for the increased potency of EACPT, as a GST inhibitor, which is able to covalently bind the Pt complex at the interface in addition to the EA moieties at the active site of the protein. Furthermore, the observation that the platinum center is later released from the interface, explains why EACPT shows an improvement in cytotoxicity when compared to cisplatin alone.

### 2.3. Overcoming GST resistance — inhibition by the metallocomplex etharapta

More recently, there has been an increasing interest in the development of metal-based drugs as effective and potent protein targeted chemotherapies [46–48]. Several ruthenium complexes are under active investigation and display a different spectrum of activity compared to platinum-based drugs [49–51]. The exact mode of cytotoxicity employed by ruthenium compounds is not fully understood but, in addition to targeting DNA, they have been shown to target specific proteins [52]. Generally, ruthenium-based drugs are much less toxic than their platinum counterparts [53,54] and thus represent a class of compounds that may be effective without displaying many of the undesirable side effects associated with platinum-based treatment.

Two drug candidates, NAMI-A and KP1019, are currently undergoing clinical evaluation against anti-metastatic tumors and colon

cancers respectively. NAMI-A shows high selectivity for solid tumor metastases and low toxicity at pharmacologically active doses and has successfully completed Phase I clinical trials [55]. KP1019 was found to be active against colorectal tumors [56] and application of therapeutic doses of the drug caused no significant toxic side effects in test animals or in patients in Phase I clinical trials [48,57].

Previously, Dyson and co-workers focused their efforts on compounds based on a series of arene capped ruthenium(II) 1,3,5-triaza-7 phosphatricyclo[3.3.1.1] decane (PTA) organometallic (RAPTA) compounds [50]. The RAPTA compounds showed strong selectivity toward a variety of cancer cell lines *in vitro* and effectively reduce lung metastasis in mice without significantly affecting the primary tumor *in vivo* and were also well tolerated [58,59]. In 2007, the same lab reported the synthesis of a series of ruthenium-based anti-cancer drugs that were shown to be significantly more cytotoxic than the platinum compound EACPT and were also effective GSTP1-1 inhibitors [60]. Etharapta, the most promising compound in the series, consists of an organometallic ruthenium center with a monodentate 1,3,5-triaza-7-phosphatricyclo [3.3.1.1]decane (PTA) ligand and an arene ligand tethered to an ethacrynic acid moiety (Fig. 1A). This compound acts as a prodrug by releasing its inhibitory EA moiety for deactivation of the GSTP1-1 enzyme while simultaneously generating a much smaller active ruthenium center for cytotoxicity.

To investigate how GSTP1-1 interacted with this compound we performed mass spectrometry and X-ray crystallographic studies [61]. Mass spectrometry showed that adducts corresponding to GST plus the whole etharapta compound (minus two chlorides) could be observed at a short exposure period of 1 h with wild-type GSTP1-1 (Fig. 1C) suggesting that the complex initially stays intact when it binds to the enzyme:

$$\mathrm{GST} + [\mathrm{EA(benzylamide)Ru(IV)(PTA)Cl_2}] \rightarrow \mathrm{GST} - [\mathrm{EA(benzylamide)Ru(II)(PTA)}] + 2\mathrm{Cl}^- . \quad (2)$$

After longer exposure times, adducts corresponding to either GST plus EA-$OH^+$ only or GST plus EA-benzylamide only were observed suggesting that the complex is cleaved and the ruthenium center is released (Fig. 1C):

$$\mathrm{GST} + [\mathrm{EA(benzylamide)Ru(IV)(PTA)Cl_2}] \rightarrow \mathrm{GST{-}EA{-}OH}^+ + [\mathrm{(benzylamide)Ru(II)(PTA)X_2}] + 2\mathrm{Cl}^- \quad (3)$$

or

$$\mathrm{GST} + [\mathrm{EA(benzylamide)Ru(IV)(PTA)Cl_2}] \rightarrow \mathrm{GST{-}EA(benzylamide)} + [\mathrm{Ru(II)(PTA)X_5}] + 2\mathrm{Cl}^- \quad (4)$$

where X represents ligands that are not definitely identified.

Although it is not clear if the enzyme plays a role in the cleavage of the complex, the release of the Ru center is required for the drug to exert its cytotoxic activity.

X-ray crystallographic studies captured views of the enzyme bound to intact and breakdown products of etharapta (Fig. 1C) [61]. X-ray data from crystals soaked with etharapta for short or long periods of time were collected. In the shorter soaks we observed a large amount of unexplained electron density at the dimer interface of the enzyme, in the same site that was identified as a binding site for the platinum center of ethacraplatin (see above) [44]. In the longer soak, however, we observed an empty dimer interface site but partially occupied substrate binding sites. (Since there are two active sites per dimer but only one EA per etharapta molecule, only half of the GST monomers in the crystal have cleaved EA bound). These data suggested that, over time, the intact etharapta is cleaved, releasing the ethacrynic acid moiety, which binds in the active site to inhibit the enzyme, as well as releasing the ruthenium center from the dimer interface binding site.

### 2.4. Conclusions

This discovery of a metal binding site at the dimer interface of GSTP1-1, has allowed us to propose a mechanism of one way that GSTP1-1 might contribute to resistance toward metal-based drugs. In turn this has shifted our focus for the design of GST inhibitors from solely targeting the active site to targeting a larger site that incorporates the dimer interface of the protein. Such inhibitors could then be used in combination therapies to prevent the excessive sequestration of anti-cancer drugs to unintended targets such as GSTP1-1 leading to improved drug efficiency. From a drug design standpoint, the selective release of an organometallic fragment by GSTP1-1 can now be exploited to deliver a variety of cytotoxic payloads for targeted chemotherapy [62].

## 3. The role of zinc in insulin-regulated aminopeptidase

### 3.1. Introduction

Insulin regulated aminopeptidase (IRAP) was originally identified as the AT4 receptor, a high affinity binding site for radiolabeled angiotensin IV (AngIV) [63]. This was a particularly important discovery as a number of AT4 ligands, including AngIV and LVV-hemophin-7 had been shown to enhance memory and cognitive functions in normal rodents when dosed intra-cranially [64,65]. Based upon the primary structure, IRAP was identified as a putative Type I transmembrane protein and a member of the zinc-dependent M1 aminopeptidase family [66]. Subsequently, the AT4 ligands were shown to be potent inhibitors of IRAP's aminopeptidase activity [63,67,68], suggesting that they may facilitate memory through the inhibition of degradation of IRAP substrates that act as endogenous neural promnesic peptides. This hypothesis was strengthened by the *in silico* development of potent, selective small molecule inhibitors of IRAP that were also able to improve cognitive function in animal models [69].

Much of the debate surrounding IRAP has centered on the mechanism behind its inhibition by the AT4 ligands. While kinetic modeling indicated that they acted as competitive inhibitors, binding to the active site [68,70], it had been observed that radiolabeled AngIV only bound to IRAP in the presence of metal chelators, suggesting that it binds to or stabilizes an apo form of the enzyme [71–73]. We thus undertook investigations into the metal binding properties of IRAP.

### 3.2. In silico approaches to identifying metal binding sites

The metal binding properties of proteins are encoded in their primary structure. The ability to predict these binding sites from the amino acid sequence can provide useful and even surprising information toward determining the function of a target protein (Fig. 2). This is particularly important where there is no significant sequence similarity to known metal-binding proteins. This task can be very challenging due to the large number of potential alternative candidate configurations. For example, a range of configurations that have been observed by X-ray crystallography can be searched in a number of available online databases (*e.g.* www.mespeus.bch.ed.ac.uk/MESPEUS_10/_1.jsp). A number of different approaches have been devised to simplify the problem.

In one approach the prediction algorithms depend upon the identification of a consensus metal-binding motif in the primary structure. A weakness of this approach is that it relies upon specific known motifs and thus cannot be applied to identify novel sites. One such database server is PROSITE (prosite.expasy.org/ [74]) which includes a range of metal-associated domain signatures and profiles. When IRAP was passed through the PROSITE server, it identified the expected consensus zinc binding [HEXXH-(18-64X)-E] and exopeptidase (GAMEN) structural motifs of the M1 aminopeptidase family.

Another approach is to predict the bonding state of selected residues, such as those available from the online server MetalDetector

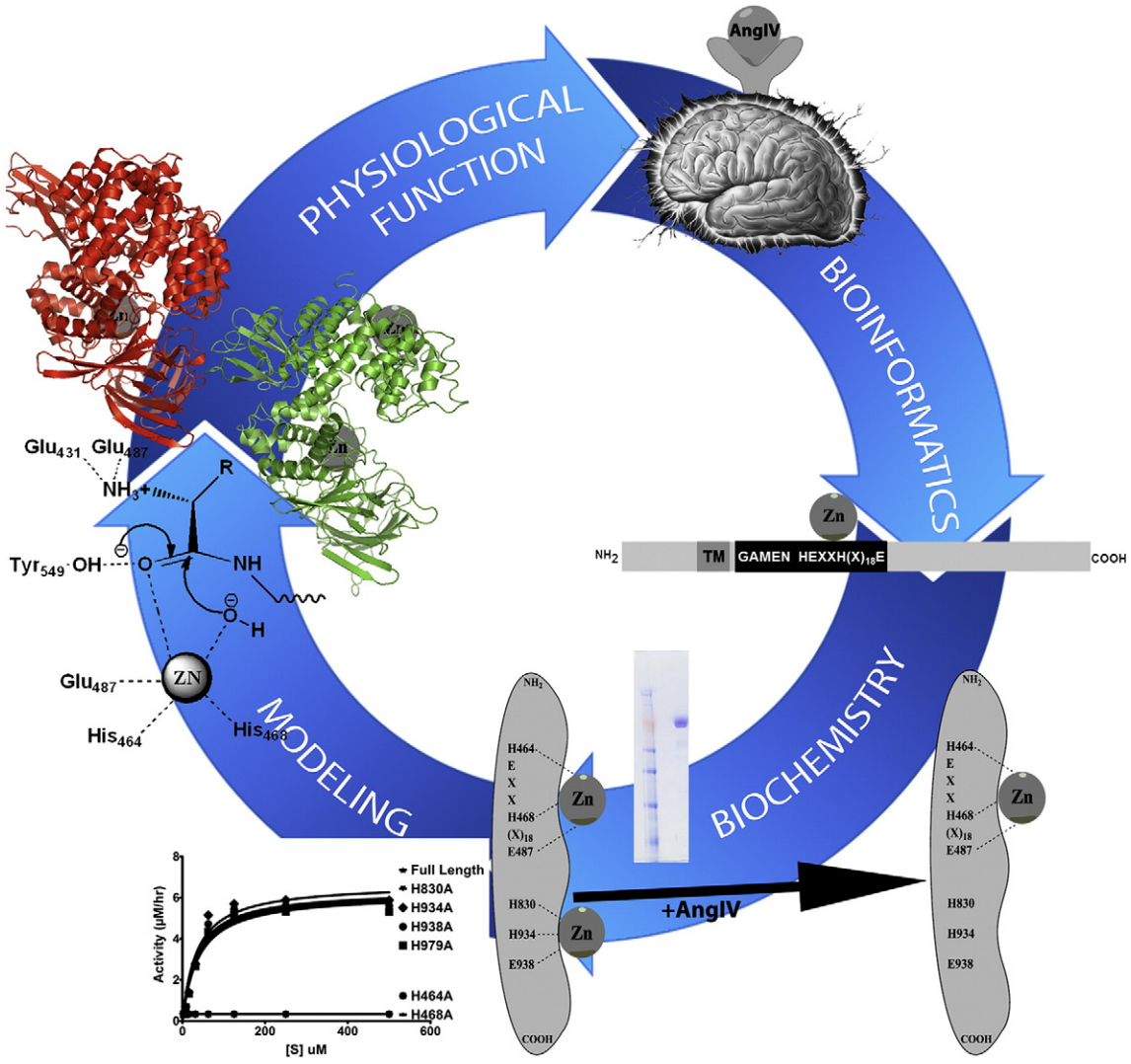


**Fig. 2.** The evolution of our understanding of the metal binding properties of IRAP. Initially observed as a specific binding site of AngIV in the brain (upper right quadrant), the primary structure revealed consensus zinc binding and aminopeptidase motifs. Recombinant expression and purification confirmed the aminopeptidase activity, and revealed two high-affinity zinc binding sites, one of which was lost upon binding of an inhibitor, AngIV (lower right quadrant). Mutagenesis was used to identify the coordinating residues. Homology modeling of IRAP in apo (green) and ligand bound (red) conformations confirmed the zinc binding biochemical observations and provided an understanding of the zinc-dependent hydrolysis, although the function of the second binding site remains unknown (left quadrants). This has allowed the understanding of the effect of mutations upon IRAP activity, and provides the foundation for the development of AngIV small molecule analogs to further explore the physiological function of IRAP and as potential therapeutics to treat dementia.

(metaldetector.dsi.unifi.it [75]) which classifies histidine residues in proteins into one of two states (free or metal bound) and cysteines into one of three states (free, metal bound or disulfide bridged). However, when IRAP was passed through the server, the software was unable to identify any putative metal-binding sites.

Advances in homology modeling have also allowed the development of servers that identify putative metal-binding sites based upon predicted three-dimensional structures. While these are limited to the accuracy of the model in question, they can be quite powerful in identifying putative sites that were not captured by the algorithms based solely upon the primary structure. MetSite (bioinf.cs.ucl.ac.uk/metsite; [76]) and FEATURE (feature.stanford.edu/metals/; [77]) are two servers that can be used to screen 3D structures including homology models for putative metal-binding sites. By using a homology model of IRAP, we were able to identify two distinct putative zinc-binding sites, the identities of which were confirmed by experimental approaches [78].

Another advantage of using modeling to characterize a metal-binding site is that it can form the basis for the development of hypotheses about likely catalytic mechanisms of action and the resulting effects of mutations. By modeling the catalytic zinc of IRAP, it was proposed that proton donation by Tyr529 completes the zinc-mediated hydrolysis of the N-terminal peptide bond of a substrate. This hypothesis explained the reduced activity of a L483F mutant, as substrate docking indicated that this crucial interaction, necessary for stabilizing a reaction intermediate, was not formed [79]. Based on the crystal structure of a related aminopeptidase, leukotriene A4 hydrolase, Leu483 was predicted to be located at the entrance of the IRAP catalytic cleft. As part of a study to define the substrate pocket of IRAP, this residue was mutated to the corresponding residue in the leukotriene A4 hydrolase and the corresponding mutant exhibited a significant reduction in activity.

### 3.3. Biochemical approaches to identifying metal binding sites

Metal ions are often important for the activity of a protein and this enables the use of biochemical assays to follow the metal dependency of a protein target. IRAP aminopeptidase activity allows its activity to be easily measured by either following the cleavage of peptide substrates by reverse-phase high performance chromatography, or in a more high-

throughput manner by following the release of a fluorophore from its amino acid conjugated precursor (for instance the release of 7-amino-4-methylcoumarin or 2-naphthylamine from the quenched substrates aminoacyl-4-methylcoumaryl-7-amides (aminoacyl-methylcoumarin) or aminoacyl-β-naphthylamide respectively):

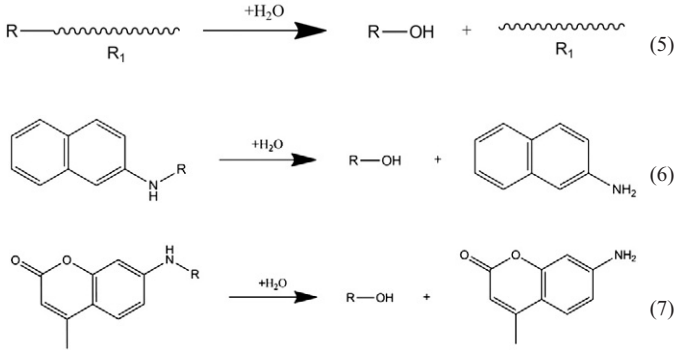


where R is commonly L-arginine, L-leucine, L-lysine or L-methionine, and $R_1$ is a peptide chain.

This allowed us to observe that IRAP was inhibited by the addition of 1,10-phenanthroline (a strong divalent metal ion chelator) but minimally by EDTA (a weaker chelator of divalent cations). This inhibition could then be reversed by the addition of zinc, supporting the prediction of a zinc-binding site based on the presence of a consensus zinc-binding aminopeptidase motif.

There are a number of traditional elemental analysis techniques, such as atomic absorption and optical emission spectrometry, including atomic emission spectroscopy, that allow the direct measurement of a range of metals. Inductively coupled plasma mass spectrometry (ICP-MS) is a more recent development that has higher throughput and better detection limits. ICP-MS combines a high-temperature ionization source (inductively coupled plasma) that converts the atoms of the sample to ions with a mass spectrometer that separates and detects the mass of these ions. While widely used for measuring metals in geochemical and physiological samples, when combined with purified protein it can be a powerful technique to identify the metal-binding properties of proteins (Fig. 2). When running purified recombinant IRAP, ICP-MS identified the presence of two zinc atoms per mole of protein, which agreed with the homology model screening described above. By utilizing a range of purified truncation constructs, the location where the two zinc ions were binding could be traced to one being in the catalytic domain and the second in a regulatory domain (Fig. 2). Examining the pH sensitivity of the binding revealed an approximate pKa of 6.2, a value that falls within the range of pKas for histidine residues, a common coordinating residue of zinc. Subsequent extensive mutagenesis of all histidines in IRAP led to identification of the coordinating histidine residues for both of these sites [78].

Not all metal binding sites in a purified recombinant protein will generally be fully occupied, even when supplemented during expression. One of our routine protocols was to strip out all metal ions from a purified protein preparation by the addition of metal chelators (*e.g.* EDTA and phenanthroline), and then reintroducing metals of interest followed by dialysis or desalting to remove unbound metal ions. In the case of IRAP we were able to confirm that both zinc-binding sites had a preference for zinc. Of the other metals tested ($Cd^{2+}$, $Cu^{2+}$, $Co^{2+}$, $Fe^{2+}$ and $Ni^{2+}$) some did show limited binding at high concentrations ($Co^{2+}$, $Cu^{2+}$ and $Ni^{2+}$) although the enzyme was inactive in all these cases (unpublished observations). By adding metal ions back in combinations, it was also observed that the presence of $Zn^{2+}$, $Ca^{2+}$ and $Mg^{2+}$ synergistically enhances the activity of IRAP [71]. (Thus in the presence of $Zn^{2+}$, addition of both $Ca^{2+}$ and $Mg^{2+}$ enhanced activity greater than by adding either alone. However, addition of either $Ca^{2+}$ or $Mg^{2+}$ only had no affect). The same approach can be taken to observe the effects of binding partners, substrates or inhibitors on the metal-binding properties of the protein. In the case of IRAP we observed that the addition of substrates or inhibitors resulted in the loss of the non-catalytic zinc [78]. This observation was proposed to be a result of the large conformational changes that the M1 aminopeptidases undergo upon binding of a substrate or inhibitor.

### 3.4. Conclusions

Metal ions can modulate the activity of proteins in many ways and we have highlighted a number of approaches to explore these interactions. There is however an important caveat in all these studies: although metal-binding can be predicted and experimentally demonstrated *in vitro* the challenge is to demonstrate their physiological relevance. For example, the identification of a non-catalytic zinc-binding site in IRAP proved enormously useful as a tool to probe the large-scale conformational changes that IRAP undergoes upon binding a substrate or inhibitor. However, the physiological relevance of the zinc-binding at this site remains to be demonstrated.

## 4. Copper in Alzheimer's disease

Metals have been implicated in Alzheimer's disease (AD), in part, through their association with the amyloid precursor protein (APP). APP is a large Type I membrane protein that is processed by a group of enzymes known as secretases. APP's large extracellular domain is shed by either α-secretase or β-secretase leaving, respectively, 83 or 99 amino acid C-terminal fragments that are sequentially processed by the integral membrane protein complex called γ-secretase. By cutting APP closer to the membrane than β-secretase, the α-secretase pathway avoids producing the amyloid-β peptide (Aβ) implicated in at least the early stage pathology of AD.

Aβ peptides vary in length (commonly 38, 40, 42 and 43 residues) according to the way they are processed at the C-terminus by γ-secretase. The longer forms of the peptide (Aβ42/Aβ43) are more prone to oligomerization/aggregation and are the major constituents of senile plaques: a pathological feature of the AD brain. The N-terminal 16 residue region of Aβ (between the β-secretase and α-secretase processing sites of APP) is known to bind zinc, copper and iron [80]. This metal binding site involves the imidazole functional groups of three histidines (Aβ residues 6, 13 and 14) and an oxygen ligand (likely from Aβ residue Asp1). Our attempts to visualize this site by crystallography of an antibody/Aβ complex were unsuccessful as the peptide was not visible beyond Ser7, while the His6 side-chain was buried in the antibody interface and therefore not available for binding metals [81]. The association of Aβ with metals via this coordination site has been implicated in Aβ oligomerization/aggregation and the production of reactive oxygen species: processes thought to contribute to the neurotoxicity of Aβ and its role in AD. The role of Aβ-metal binding in AD is complex and comprehensively reviewed elsewhere [80–83].

Here we focus on our studies of the interaction between copper and a second high affinity metal binding site in the cysteine-rich N-terminal region of APP, and discuss the potential to target this copper binding domain (CuBD) in AD therapeutic development. Of particular interest here is that in our studies of the APP CuBD, we have applied several biophysical techniques to describe this protein–metal interaction including solution state NMR spectroscopy, EPR, X-ray crystallography and EXAFS.

The neuronal isoform of APP shown in Fig. 3A has a cysteine-rich N-terminal E1 region connected to a structured E2 region by a low complexity acidic domain. There is a putative random coil region (D6b; Fig. 3A) following the helical E2 domain and preceding the membrane (TM; Fig. 3A) and a short intracellular portion (IC; Fig. 3A). In 1999 we solved the first high resolution APP crystal structure (PDB ID:

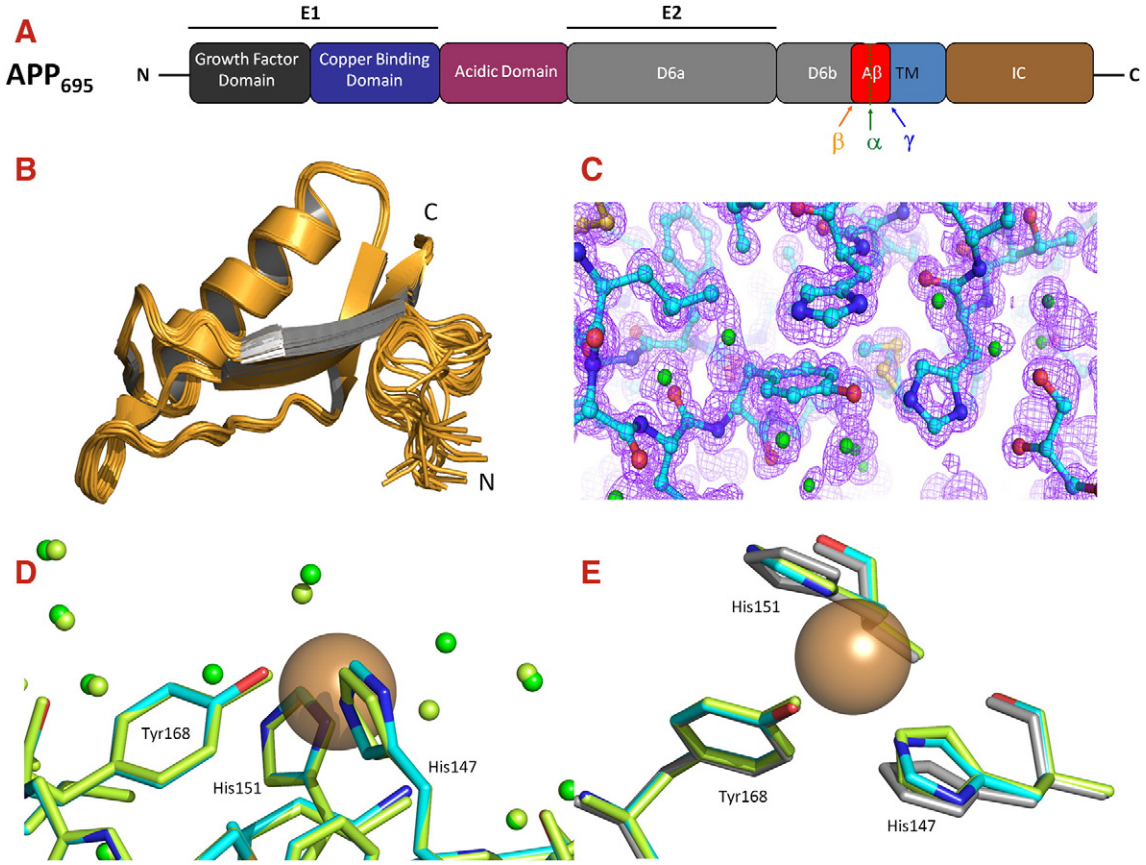


**Fig. 3.** Copper binding to APP. (A) A cartoon representation of the 695 residue neuronal isoform of APP. The region of Aβ is colored in red, with the three secretase proteolytic sites marked. TM indicates the transmembrane domain. (B) 3D structures of the APP copper binding domain — the 21 lowest-energy solution-state structures derived by NMR restraints, superpositioned across backbone heavy atoms. (C) Ultra-high resolution (0.85 Å) model and electron density map derived by X-ray crystallography, highlighting atomic resolution and exceptional visualization of side-chains and water. (D) APP CuBD structures determined by X-ray crystallography bound to $Cu^{2+}$ (protein colored by atom type and waters colored green) and bound to $Cu^{+}$ (colored lemon). (E) The same as in panel D but with the unliganded CuBD structure shown in gray. Note the difference in water occupancy and slight histidine rearrangements in panels D and E. Also note that $Cu^{2+}$ ion positions are shown as copper colored spheres.

1MWP; [84]): the N-terminal growth factor-like domain (GFD, residues 28–123) that binds heparin, and stimulates neurite outgrowth [85] amongst other things. From a structural perspective, it was interesting that the N-terminal GFD proved to be an independently folded domain, yet constituted only part of the cysteine-rich E1 region. This suggested that the remaining portion of E1, namely the copper binding domain, could likewise form an independently folded domain.

The functions of APP are not fully known, but some key observations of APP behavior relevant to AD pathology provided the imperative to study the structure of the APP CuBD: (a) extracellular $Cu^{2+}$ treatment of CHO cells over-expressing APP shifts the equilibrium of APP processing away from the amyloidogenic β-/γ-secretase pathway toward the non-amyloidogenic α-/γ-secretase pathway, thereby reducing Aβ peptide production [86]; (b) this effect is abolished when the copper binding histidine residues in the CuBD are mutated [87]; (c) APP is important in neuronal copper homeostasis (APP knockout mice have increased copper levels in the brain, while APP-over-expressing mice have reduced brain copper) [88,89]; (d) APP can reduce $Cu^{2+}$ to $Cu^{+}$ *in vitro* suggesting a potential role for APP in copper-mediated free radical production [90]; and (e) the isolated CuBD showed similar copper binding and redox activity to intact APP [91].

Initial attempts to crystallize the CuBD (APP residues 124–189) were unsuccessful. However, this construct proved amenable to 3D structure determination in the apo form by solution state NMR (PDB ID: 1OWT; [92]). The 21 lowest energy models of the CuBD calculated from NMR-derived restraints are shown in Fig. 3B. The structures show an α-helix (APP residues 147–159) sitting across a β-sheet of three strands (APP residues 133–139, 162–167 and 181–188). The structure was stabilized by three disulfide bonds between the APP residue pairs Cys133–Cys187, Cys158–Cys186 and Cys144–Cys174. The final 21 structures were well ordered across APP residues 127–189 with a root mean square difference across backbone heavy atoms of 0.4 Å, with only the first 3 amino acids unstructured. A phenomenon where resonances from nuclei in close proximity to a paramagnetic center such as Cu(II) are broadened in the NMR spectrum was exploited to identify APP residues His147, His151, Tyr168 and Met170 as the Cu(II) ligands in the CuBD. EPR data reported in the Barnham et al. [92] paper on an N-terminally truncated CuBD construct (residues 133–189) were consistent with a coordination sphere about Cu(II) intermediate between a square planar and a tetrahedral geometry preferred by Cu(II) and Cu(I), respectively.

The paramagnetic resonance broadening effect, while useful in identifying Cu(II) ligands, also broadens resonances such that structural data for ligating residues is lost. We exploited the ensemble of NMR-derived models to design a new CuBD construct (APP residues 133–189) for crystallization experiments, lacking the N-terminal region which is highly mobile and potentially inhibitory to crystallization. This strategy ultimately led to the successful crystallization and structure determination of the apo form of the CuBD to a resolution of 0.85 Å (PDB ID: 2FMA; [93]), shown in Fig. 3C. Furthermore, we were able to successfully obtain high resolution structures of the CuBD bound to $Cu^{2+}$ and to $Cu^{+}$ (PDB ID: 2FK1 and 2FK2, respectively; [94]) in which the ligands adopt distorted pyramidal and distorted square planar geometries, respectively (see Fig. 3D and E). The CuBD:$Cu^{2+}$ shows $Cu^{2+}$ coordinated by $N_{\varepsilon}2$ of His147, $N_{\delta}1$ of His151, the hydroxyl oxygen of

Tyr168 and two waters above the plane of amino acid ligand atoms. This geometry is consistent with EPR and with analysis of EXAFS data collected from a frozen solution of the CuBD:$Cu^{2+}$ complex confirming that the coordinating ligands and their geometry around the metal site were retained in the crystalline state. The CuBD:$Cu^{+}$ structure is similar to the CuBD:$Cu^{2+}$ minus a coordinating water and slight re-orientation of the side-chains of His147 and His151. These structures superimpose well with the NMR-derived solution state structures. The crystallography revealed that Met170 was not a ligand to the metal with the sulfur atom 7 Å distant from the metal ion. However, we proposed that Met170 may play an important role as an electron donor to $Cu^{2+}$, either through rapid conformational changes which would bring the sulfur atom in close contact with the metal ion, or through an electron transfer pathway which relays the electron from Met170 to $Cu^{2+}$:

$$\mathrm{CuBD/Met170_{Red}} + \mathrm{Cu^{2+}} \rightarrow \mathrm{CuBD/Met170_{Ox}} + \mathrm{Cu^{+}} \quad (8)$$

The multidisciplinary strategy taken to characterize the CuBD of APP led us to develop an atomic resolution mechanism for the reduction of Cu(II) by APP, and explain the redox activity of APP and its contribution to copper homeostasis as a metallochaperone. The ultra-high resolution model of the CuBD provides a template for the design of inhibitors of this redox center if its role in copper-mediated free radical production is proven important to the pathology of AD or related disorders. What our structures do not explain is how $Cu^{2+}$ can shift the equilibrium of APP processing away from the amyloidogenic pathway toward the non-amyloidogenic pathway, thereby modulating Aβ peptide production [86,87]. Copper binding to the CuBD leads to slight and local conformational changes only in the monomeric structures. The observation by Scheuermann et al. [95] that forced homodimerization of APP increases the production of Aβ, led us to hypothesize that in the context of intact APP, co-operative copper binding might modulate APP oligomerization, and thereby modulate Aβ production. If substantiated, this could open the way for the development of therapeutics that modulate Aβ production by targeting the CuBD of APP.

## 5. XAS in health and disease

The structural characterization of metal-binding interactions with metalloenzymes using X-ray absorption spectroscopy is well established in the bioinorganic literature and the advantages of using the technique to complement X-ray crystallographic and other information are evident in the examples discussed above. Despite the fact that it is a relatively information-poor technique, the "phase agnostic" nature of XAS means that it is especially useful in identifying situations where other biophysical techniques have resulted in perturbation from the physiologically relevant setting. While we have used XANES in the EACPT–GST binding study discussed above to establish the reduction of Pt in ethacraplatin on interaction with GST, the complementary utility of XAS is better demonstrated by our work on $Cu^{2+}$ interacting with APP. In that work we confirm the physiological relevance of the X-ray diffraction structural analysis for $Cu^{2+}$ bound to APP in the crystalline state by using EXAFS to structurally characterize the complex in solution, a more physiologically relevant situation obviously inaccessible to diffraction studies, and demonstrate that the metal-binding geometries from the two approaches were in agreement.

Another significant advantage of XAS is that the X-ray dose required to acquire acceptable quality data can be orders of magnitude lower than that required for crystallographic structure determination of metalloproteins, meaning that the risk of damaging the chemistry of the metal center under study by the act of measurement itself is significantly lower. This was perhaps best illustrated by Yano et al. [96] who demonstrated, using EXAFS analysis of a single crystal of photosystem-II, that the structure of the Mn4Ca cluster at the active site of the enzyme was seriously affected by an X-ray dose an order of magnitude lower than that normally considered "safe" for X-ray crystallographic studies. Their study also elegantly illustrates both the exquisite sensitivity of XANES to act as a marker of chemical changes at metalloprotein active sites without the requirement for significant analysis and, in comparison to our experiments on frozen solutions described above, the ability of the method to cope with samples in any form.

It is not difficult to envisage how XAS could be used to expand our knowledge of the other systems described here. For instance, Ru K-edge XANES of etharapta and related complexes interacting with GST in either the solution or crystalline states, would reveal the time evolution of the redox state of the bound metal ion; information which is potentially central to understanding the action of the drug *in vivo*. In addition, analysis of the EXAFS for the same systems could confirm the results of the crystallographic results already published. Similarly, Zn K-edge EXAFS could be employed to elucidate the binding of Zn to IRAP by determining its binding geometry in the native recombinant protein as well as in truncation constructs. In this situation, multiple-scattering EXAFS analysis could be used to confirm the number of histidine ligands coordinated to Zn in a manner identical to that used by George et al. [97].

In some situations a "top-down" XAS approach, taking advantage of the "phase agnostic" and element specific characteristics of the method, can be employed to guide traditional "bottom-up" biochemical experiments in understanding how metal ions interact with proteins and other biomolecules. This is especially true for exogenous metal ions, such as those in various metal-based drugs, where there is no background from the existing pool of metals in the system. An example of this has demonstrated, using XANES of cultured cell pellets, that the distribution of Cr species in cultured cells treated with Cr(VI) is altered by standard cellular fractionation [98]. The resultant implication was that the identification of the species on which the dietary essentiality of Cr is based, chromodulin, may in fact be an artifact of its isolation procedure. This approach is not limited to cultured cells but can also be applied to whole tissues from animals treated with similar species.

## 6. Concluding remarks

We have described a number of biophysical tools used to characterize metal-binding interactions with proteins including mass spectrometry, bioinformatics, computational modeling, NMR, EPR, X-ray crystallography, XANES and EXAFS. In each case the complementarity of the techniques in exploring a biological problem has been highlighted. Indeed it was shown that a multi-pronged approach was essential to provide a more complete understanding of the biology behind each case study. We also highlighted an important caveat: although metal-binding can be experimentally demonstrated *in vitro*, the challenge is then to show the physiological relevance of such binding.

*Table of abbreviations*

| | |
|---|---|
| Aβ | peptide associated with Alzheimer's disease |
| AD | Alzheimer's disease |
| AngIV | angiotensin IV |
| APP | amyloid precursor protein |
| AT4 | angiotensin IV |
| CPT | cisplatin |
| CuBD | copper binding domain of amyloid precursor protein |
| EA | ethacrynic acid |
| EACPT | ethacraplatin |
| EXAFS | extended X-ray absorption fine structure spectroscopy |
| GFD | growth factor domain of amyloid precursor protein |
| GSH | glutathione |
| GST | glutathione S-transferase |
| GSTP1-1 | pi class isoform of GST |

| | |
|---|---|
| ICP-MS | inductively coupled plasma mass spectrometry |
| IRAP | insulin regulated aminopeptidase |
| PTA | 1,3,5-triaza-7 phosphatricyclo[3.3.1.1] decane |
| RAPTA | arene capped ruthenium(II) 1,3,5-triaza-7 phosphatricyclo [3.3.1.1] decane |
| XANES | X-ray absorption near edge structure |
| XAS | X-ray absorption spectroscopy |

## Acknowledgments

We thank all present and past staff of BSBL and our collaborators for all their contributions toward the studies highlighted in this review. Infrastructure support from the National Health and Medical Research Council Independent Research Institutes Infrastructure Support Scheme and the Victorian State Government Operational Infrastructure Support Program is gratefully acknowledged. L.J.P. was supported by a National Health and Medical Research Council of Australia (NHMRC) Dora Lush Scholarship and an International Centre for Diffraction Data Crystallography Scholarship. D.B.A. was an Australian Postgraduate Award Scholar and the recipient of a St. Vincent's Institute Foundation Scholarship sponsored by Colin North and Major Engineering. C.G. is an Australian Postgraduate Award Scholar. H.H.H. is an Australian Research Council Queen Elizabeth II fellow and M.W.P. is an Australian Research Council Federation fellow and NHMRC honorary fellow.

## References

[1] P.M. Colman, H.C. Freeman, J.M. Guss, M. Murata, V.A. Norris, J.A.M. Ramshaw, M.P. Venkatappa, Nature 272 (1978) 319–324.
[2] M.W. Parker, Aust. N. Z. J. Med. 25 (1995) 876–882.
[3] D. Sheehan, G. Meade, V.M. Foley, C.A. Dowd, Biochem. J. 360 (2001) 1–16.
[4] M.C. Wilce, M.W. Parker, Biochim. Biophys. Acta 1205 (1994) 1–18.
[5] J. Rossjohn, S.C. Feil, M.C. Wilce, J.L. Sexton, T.W. Spithill, M.W. Parker, J. Mol. Biol. 273 (1997) 857–872.
[6] B. Mannervik, P.G. Board, J.D. Hayes, I. Listowsky, W.R. Pearson, Methods Enzymol. 401 (2005) 1–8.
[7] C. Frova, Biomol. Eng. 23 (2006) 149–169.
[8] B. Mannervik, Y.C. Awasthi, P.G. Board, J.D. Hayes, C. Di Ilio, B. Ketterer, I. Listowsky, R. Morgenstern, M. Muramatsu, W.R. Pearson, et al., Biochem. J. 282 (Pt 1) (1992) 305–306.
[9] H. Ranson, L. Rossiter, F. Ortelli, B. Jensen, X. Wang, C.W. Roth, F.H. Collins, J. Hemingway, Biochem. J. 359 (2001) 295–304.
[10] T. Inoue, T. Ishida, K. Sugio, Y. Maehara, K. Sugimachi, Respiration 62 (1995) 223–227.
[11] K. Sato, Adv. Cancer Res. 52 (1989) 205–255.
[12] M.J. Ruiz-Gomez, A. Souviron, M. Martinez-Morillo, L. Gil, J. Physiol. Biochem. 56 (2000) 307–312.
[13] J.A. Green, L.J. Robertson, A.H. Clark, Br. J. Cancer 68 (1993) 235–239.
[14] A. Katagiri, Y. Tomita, T. Nishiyama, M. Kimura, S. Sato, Br. J. Cancer 68 (1993) 125–129.
[15] S.V. Singh, B.H. Xu, V. Gupta, E.O. Emerson, H.A. Zaren, J.P. Jani, Cancer Lett. 95 (1995) 49–56.
[16] L. Zhang, Y. Xiao, R. Priddy, J. Oral Pathol. Med. 23 (1994) 75–79.
[17] D.J. Grignon, M. Abdel-Malak, W.C. Mertens, W.A. Sakr, R.R. Shepherd, Mod. Pathol. 7 (1994) 186–189.
[18] M. O'Brien, G.D. Kruh, K.D. Tew, J. Pharmacol. Exp. Ther. 294 (2000) 480–487.
[19] J.D. Hayes, C.R. Wolf, Biochem. J. 272 (1990) 281–295.
[20] K.D. Tew, A.M. Bomber, S.J. Hoffman, Cancer Res. 48 (1988) 3622–3625.
[21] P.J. O'Dwyer, F. LaCreta, S. Nash, P.W. Tinsley, R. Schilder, M.L. Clapper, K.D. Tew, L. Panting, S. Litwin, R.L. Comis, et al., Cancer Res. 51 (1991) 6059–6065.
[22] M. Petrini, A. Conte, F. Caracciolo, A. Sabbatini, B. Grassi, G. Ronca, Br. J. Haematol. 85 (1993) 409–410.
[23] B. Rosenberg, L. Vancamp, T. Krigas, Nature 205 (1965) 698–699.
[24] R.B. Weiss, M.C. Christian, Drugs 46 (1993) 360–377.
[25] G. Giaccone, Drugs 59 (Suppl 4) (2000) 9–17 (and discussion 37-18).
[26] E. Wong, C.M. Giandomenico, Chem. Rev. 99 (1999) 2451–2466.
[27] J. Reedijk, Chem. Commun. (1996) 801–806.
[28] G. Chu, J. Biol. Chem. 269 (1994) 787–790.
[29] V. Cepeda, M.A. Fuertes, J. Castilla, C. Alonso, C. Quevedo, J.M. Perez, Anticancer Agents Med Chem. 7 (2007) 3–18.
[30] M.A. Fuertes, C. Alonso, J.M. Perez, Chem. Rev. 103 (2003) 645–662.
[31] H. Oguchi, F. Kikkawa, M. Kojima, O. Maeda, K. Mizuno, N. Suganuma, M. Kawai, Y. Tomoda, Anticancer Res. 14 (1994) 193–200.
[32] T. Yasuno, T. Matsumura, T. Shikata, J. Inazawa, T. Sakabe, S. Tsuchida, T. Takahata, S. Miyairi, A. Naganuma, T. Sawada, Anticancer Res. 19 (1999) 4049–4057.
[33] S. Tsuchida, K. Sato, Crit. Rev. Biochem. Mol. Biol. 27 (1992) 337–384.
[34] G. Ferrandina, G. Scambia, G. Damia, G. Tagliabue, A. Fagotti, P. Benedetti Panici, C. Mangioni, S. Mancuso, M. D'Incalci, Ann. Oncol. 8 (1997) 343–350.
[35] T. Nakajima, T. Takayama, K. Miyanishi, A. Nobuoka, T. Hayashi, T. Abe, J. Kato, K. Sakon, Y. Naniwa, H. Tanabe, Y. Niitsu, J. Pharmacol. Exp. Ther. 306 (2003) 861–869.
[36] C.R. Wolf, B.K. Park, N. Kitteringham, D. Otto, C.H. Henderson, Chem. Biol. Interact. 133 (2001) 280–284.
[37] M.D. Hall, T.W. Hambley, Coord. Chem. Rev. 232 (2002) 49–67.
[38] G.K. Poon, P. Mistry, F.I. Raynaud, K.R. Harrap, B.A. Murrer, C.F. Barnard, J. Pharm. Biomed. Anal. 13 (1995) 1493–1498.
[39] P. Sova, A. Mistr, A. Kroutil, F. Zak, P. Pouckova, M. Zadinova, Anticancer Drugs 16 (2005) 653–657.
[40] A. Kozubik, V. Horvath, L. Svihalkova-Sindlerova, K. Soucek, J. Hofmanova, P. Sova, A. Kroutil, F. Zak, A. Mistr, J. Turanek, Biochem. Pharmacol. 69 (2005) 373–383.
[41] J. Kasparkova, O. Novakova, O. Vrana, F. Intini, G. Natile, V. Brabec, Mol. Pharmacol. 70 (2006) 1708–1719.
[42] W.H. Ang, I. Khalaila, C.S. Allardyce, L. Juillerat-Jeanneret, P.J. Dyson, J. Am. Chem. Soc. 127 (2005) 1382–1383.
[43] W.H. Ang, S. Pilet, R. Scopelliti, F. Bussy, L. Juillerat-Jeanneret, P.J. Dyson, J. Med. Chem. 48 (2005) 8060–8069.
[44] L.J. Parker, L.C. Italiano, C.J. Morton, N.C. Hancock, D.B. Ascher, J.B. Aitken, H.H. Harris, P. Campomanes, U. Rothlisberger, A. De Luca, M. Lo Bello, W.H. Ang, P.J. Dyson, M.W. Parker, Chem. Eur. J. 17 (2011) 7806–7816.
[45] A.J. Oakley, J. Rossjohn, M. Lo Bello, A.M. Caccuri, G. Federici, M.W. Parker, Biochemistry 36 (1997) 576–585.
[46] R. Alberto, C. Biot, A. Casini, D. Dive, P.J. Dyson, S. Gibaud, A. Habtermariam, C.G. Hartinger, E.A. Hillard, M. Hogan, G. Jaouen, B.E. Mann, E. Meggers, S.P. Mulcahy, A.A. Nazarov, N. Metzler-Nolte, A.M. Pizarro, P.J. Sadler, M. Tacke, A. Vessieres, Medicinal Organometallic Chemistry: Topics in Organometallic Chemistry, 32, Springer-Verlag, 2010.
[47] C.S. Allardyce, A. Dorcier, C. Scolaro, P.J. Dyson, Appl. Organomet. Chem. 19 (2005) 1–10.
[48] M.A. Jakupec, M. Galanski, V.B. Arion, C.G. Hartinger, B.K. Keppler, Dalton Trans. (2008) 183–194.
[49] W.H. Ang, E. Daldini, C. Scolaro, R. Scopelliti, L. Juillerat-Jeannerat, P.J. Dyson, Inorg. Chem. 45 (2006) 9006–9013.
[50] C. Scolaro, A. Bergamo, L. Brescacin, R. Delfino, M. Cocchietto, G. Laurenczy, T.J. Geldbach, G. Sava, P.J. Dyson, J. Med. Chem. 48 (2005) 4161–4171.
[51] C.A. Vock, C. Scolaro, A.D. Phillips, R. Scopelliti, G. Sava, P.J. Dyson, J. Med. Chem. 49 (2006) 5552–5561.
[52] E. Alessio, G. Mestroni, A. Bergamo, G. Sava, Met. Ions Biol. Syst. 42 (2004) 323–351.
[53] R.E. Yasbin, C.R. Matthews, M.J. Clarke, Chem. Biol. Interact. 31 (1980) 355–365.
[54] M. Galanski, V.B. Arion, M.A. Jakupec, B.K. Keppler, Curr. Pharm. Des. 9 (2003) 2078–2089.
[55] J.M. Rademaker-Lakhai, D. van den Bongard, D. Pluim, J.H. Beijnen, J.H. Schellens, Clin. Cancer Res. 10 (2004) 3717–3727.
[56] M.H. Seelig, M.R. Berger, B.K. Keppler, J. Cancer Res. Clin. Oncol. 118 (1992) 195–200.
[57] C.G. Hartinger, S. Zorbas-Seifried, M.A. Jakupec, B. Kynast, H. Zorbas, B.K. Keppler, J. Inorg. Biochem. 100 (2006) 891–904.
[58] P.J. Dyson, G. Sava, Dalton Trans. (2006) 1929–1933.
[59] M. Melchart, P.J. Sadler, Bioorganometallics: Chapter 2. Ruthenium Arene Anticancer Complexes, Wiley-VCH, Weinheim, Germany, 2006.
[60] W.H. Ang, A. De Luca, C. Chapuis-Bernasconi, L. Juillerat-Jeanneret, M. Lo Bello, P.J. Dyson, ChemMedChem 2 (2007) 1799–1806.
[61] W.H. Ang, L.J. Parker, A. De Luca, L. Juillerat-Jeanneret, C.J. Morton, M. Lo Bello, M.W. Parker, P.J. Dyson, Angew. Chem. Int. Ed Engl. 48 (2009) 3854–3857.
[62] K.D. Tew, Expert Opin. Investig. Drugs 14 (2005) 1047–1054.
[63] A.L. Albiston, S.G. McDowall, D. Matsacos, P. Sim, E. Clune, T. Mustafa, J. Lee, F.A. Mendelsohn, R.J. Simpson, L.M. Connolly, S.Y. Chai, J. Biol. Chem. 276 (2001) 48623–48626.
[64] J.W. Wright, A.V. Miller-Wing, M.J. Shaffer, C. Higginson, D.E. Wright, J.M. Hanesworth, J.W. Harding, Brain Res. Bull. 32 (1993) 497–502.
[65] J.W. Wright, L. Stubley, E.S. Pederson, E.A. Kramar, J.M. Hanesworth, J.W. Harding, J. Neurosci. 19 (1999) 3952–3961.
[66] T. Rogi, M. Tsujimoto, H. Nakazato, S. Mizutani, Y. Tomoda, J. Biol. Chem. 271 (1996) 56–61.
[67] J. Lee, T. Mustafa, S.G. McDowall, F.A. Mendelsohn, M. Brennan, R.A. Lew, A.L. Albiston, S.Y. Chai, J. Pharmacol. Exp. Ther. 305 (2003) 205–211.
[68] R.A. Lew, T. Mustafa, S. Ye, S.G. McDowall, S.Y. Chai, A.L. Albiston, J. Neurochem. 86 (2003) 344–350.
[69] A.L. Albiston, C.J. Morton, H.L. Ng, V. Pham, H.R. Yeatman, S. Ye, R.N. Fernando, D. De Bundel, D.B. Ascher, F.A. Mendelsohn, M.W. Parker, S.Y. Chai, FASEB J. 22 (2008) 4209–4217.
[70] S. Ye, S.Y. Chai, R.A. Lew, A.L. Albiston, Biol. Chem. 388 (2007) 399–403.
[71] H. Demaegdt, H. Laeremans, J.P. De Backer, S. Mosselmans, M.T. Le, V. Kersemans, Y. Michotte, G. Vauquelin, P.M. Vanderheyden, Biochem. Pharmacol. 68 (2004) 893–900.
[72] H. Demaegdt, P.J. Lenaerts, J. Swales, J.P. De Backer, H. Laeremans, M.T. Le, K. Kersemans, L.K. Vogel, Y. Michotte, P. Vanderheyden, G. Vauquelin, Eur. J. Pharmacol. 546 (2006) 19–27.
[73] H. Demaegdt, A. Lukaszuk, E. De Buyser, J.P. De Backer, E. Szemenyei, G. Toth, S. Chakravarthy, M. Panicker, Y. Michotte, D. Tourwe, G. Vauquelin, Mol. Cell. Endocrinol. 311 (2009) 77–86.
[74] C.J. Sigrist, L. Cerutti, E. de Castro, P.S. Langendijk-Genevaux, V. Bulliard, A. Bairoch, N. Hulo, Nucleic Acids Res. 38 (2010) D161–166.

[75] M. Lippi, A. Passerini, M. Punta, B. Rost, P. Frasconi, Bioinformatics 24 (2008) 2094–2095.
[76] J.S. Sodhi, K. Bryson, L.J. McGuffin, J.J. Ward, L. Wernisch, D.T. Jones, J. Mol. Biol. 342 (2004) 307–320.
[77] J.C. Ebert, R.B. Altman, Protein Sci. 17 (2008) 54–65.
[78] D.B. Ascher, B.A. Cromer, C.J. Morton, I. Volitakis, R.A. Cherny, A.L. Albiston, S.Y. Chai, M.W. Parker, Biochemistry 50 (2011) 2611–2622.
[79] S. Ye, S.Y. Chai, R.A. Lew, D.B. Ascher, C.J. Morton, M.W. Parker, A.L. Albiston, Biochem. Cell Biol. 86 (2008) 251–261.
[80] J.A. Duce, A.I. Bush, P.A. Adlard, Future Neurol. 6 (2011) 641–659.
[81] L.A. Miles, K.S. Wun, G.A. Crespi, M.T. Fodero-Tavoletti, D. Galatis, C.J. Bagley, K. Beyreuther, C.L. Masters, R. Cappai, W.J. McKinstry, K.J. Barnham, M.W. Parker, J. Mol. Biol. 377 (2008) 181–192.
[82] A. Rauk, Chem. Soc. Rev. 38 (2009) 2698–2715.
[83] M. Rozga, W. Bal, Chem. Res. Toxicol. 23 (2010) 298–308.
[84] J. Rossjohn, R. Cappai, S.C. Feil, A. Henry, W.J. McKinstry, D. Galatis, L. Hesse, G. Multhaup, K. Beyreuther, C.L. Masters, M.W. Parker, Nat. Struct. Biol. 6 (1999) 327–331.
[85] I. Ohsawa, C. Takamura, S. Kohsaka, Biochem. Biophys. Res. Commun. 236 (1997) 59–65.
[86] T. Borchardt, J. Camakaris, R. Cappai, C.L. Masters, K. Beyreuther, G. Multhaup, Biochem. J. 344 (Pt 2) (1999) 461–467.
[87] T. Borchardt, C. Schmidt, J. Camarkis, R. Cappai, C.L. Masters, K. Beyreuther, G. Multhaup, Cell. Mol. Biol. (Noisy-le-Grand) 46 (2000) 785–795.
[88] A.R. White, R. Reyes, J.F. Mercer, J. Camakaris, H. Zheng, A.I. Bush, G. Multhaup, K. Beyreuther, C.L. Masters, R. Cappai, Brain Res. 842 (1999) 439–444.
[89] C.J. Maynard, R. Cappai, I. Volitakis, R.A. Cherny, A.R. White, K. Beyreuther, C.L. Masters, A.I. Bush, Q.X. Li, J. Biol. Chem. 277 (2002) 44670–44676.
[90] G. Multhaup, A. Schlicksupp, L. Hesse, D. Beher, T. Ruppert, C.L. Masters, K. Beyreuther, Science 271 (1996) 1406–1409.
[91] A.R. White, G. Multhaup, D. Galatis, W.J. McKinstry, M.W. Parker, R. Pipkorn, K. Beyreuther, C.L. Masters, R. Cappai, J. Neurosci. 22 (2002) 365–376.
[92] K.J. Barnham, W.J. McKinstry, G. Multhaup, D. Galatis, C.J. Morton, C.C. Curtain, N.A. Williamson, A.R. White, M.G. Hinds, R.S. Norton, K. Beyreuther, C.L. Masters, M.W. Parker, R. Cappai, J. Biol. Chem. 278 (2003) 17401–17407.
[93] G.K. Kong, J.J. Adams, R. Cappai, M.W. Parker, Acta Crystallogr. Sect. F Struct. Biol. Cryst. Commun. 63 (2007) 819–824.
[94] G.K. Kong, J.J. Adams, H.H. Harris, J.F. Boas, C.C. Curtain, D. Galatis, C.L. Masters, K.J. Barnham, W.J. McKinstry, R. Cappai, M.W. Parker, J. Mol. Biol. 367 (2007) 148–161.
[95] S. Scheuermann, B. Hambsch, L. Hesse, J. Stumm, C. Schmidt, D. Beher, T.A. Bayer, K. Beyreuther, G. Multhaup, J. Biol. Chem. 276 (2001) 33923–33929.
[96] J. Yano, J. Kern, K.D. Irrgang, M.J. Latimer, U. Bergmann, P. Glatzel, Y. Pushkar, J. Biesiadka, B. Loll, K. Sauer, J. Messinger, A. Zouni, V.K. Yachandra, Proc. Natl. Acad. Sci. U. S. A. 102 (2005) 12047–12052.
[97] G.C. Ferreira, R. Franco, A. Mangravita, G.N. George, Biochemistry 41 (2002) 4809–4818.
[98] A. Levina, H.H. Harris, P.A. Lay, J. Am. Chem. Soc. 129 (2007) 1065–1075.